Pigment Organization Effects on Energy Transfer and Chl a Emission Imaged in the Diatoms C. meneghiniana and P. tricornutum In Vivo: A Confocal Laser Scanning Fluorescence (CLSF) M...

ARTICLE *in* THE JOURNAL OF PHYSICAL CHEMISTRY B · JULY 2013

Impact Factor: 3.3 · DOI: 10.1021/jp402094c · Source: PubMed

THE JOURNAL OF PHYSICAL CHEMISTRY B

Article

pubs.acs.org/JPCB

Pigment Organization Effects on Energy Transfer and *Chl a* Emission Imaged in the Diatoms *C. meneghiniana* and *P. tricornutum* In Vivo: A Confocal Laser Scanning Fluorescence (CLSF) Microscopy and Spectroscopy Study

Lavanya Premvardhan,*[,†] Matthieu Réfrégiers,[†] and Claudia Büchel*[,‡]

[†]Synchrotron SOLEIL, L'Ormes des Merisiers, Saint Aubin BP 48, 91192 Gif/Yvette Cedex, France

[‡]Institute of Molecular Biosciences, Goethe University, Frankfurt, Germany

Supporting Information

ABSTRACT: The (auto)fluorescence from three diatom strains, *Cyclotella meneghiniana* (*Cm*), *Phaeodactylum tricornutum 1a* (*Pt1a*), and *Phaeodactylum UTex* (*PtUTex*), has been imaged in vivo to submicrometer resolution using confocal laser scanning fluorescence (CLSF) microscopy. The diatoms are excited at 473 and 532 nm, energy primarily absorbed by the carotenoid fucoxanthin (*Fx*) found within the fucoxanthin chlorophyll *a*/*c* proteins (FCPs). On the basis of the fluorescence spectra measured in each image voxel, we obtain information about the spatial and energetic distribution of the terminal *Chl a* emitters, localized in the FCPs and the reaction centers of the PSII protein complexes, and the nature and location of the primary absorbers that are linked to these emitters; 532 nm excites the highly efficient Fx_{red} light harvesters, and lesser amounts of Fx_{green}s, that are enriched in some FCPs and preferentially transfer energy to PSII, compared to 473 nm, which excites almost equal amounts of all three previously identified sets of *Fx* − Fx_{red}, Fx_{green} and Fx_{blue} − as well as *Chl c*. The heterogeneous *Chl a* emission observed from the (C)LSF images indicates that the different *Fx*'s serve different final emitters in *P. tricornutum* and suggest, at least in *C. meneghiniana*, a localization of FCPs with relatively greater Fx_{red} content at the chloroplast edges, but with overall higher FCP concentration in the interior of the plastid. To better understand our results, the concentration-dependent ensemble-averaged diatom solution spectra are compared to the (auto)fluorescence spectra of individual diatoms, which indicate that pigment packing effects at an intracellular level do affect the diatoms' spectral properties, in particular, concerning a 710 nm emission band apparent under stress conditions. A species-specific response of the spectral signature to the incident light is also discussed in terms of the presence of a silica shell in *Cm* but not in *Pt1a* nor *PtUTex*.

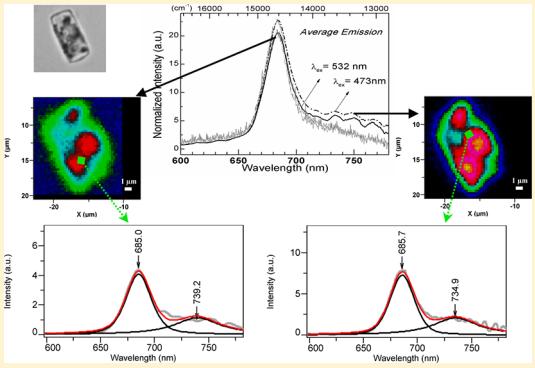

INTRODUCTION

Life on earth is supported by oxygenic photosynthesis, about 50% of which originates from marine (and freshwater) phytoplankton although they account for only about 1% of total photosynthetic biomass.[1,2] Among these phytoplankton, eukaryotic diatoms such as *Cyclotella meneghiniana* (*Cm*) and *Phaeodactylum tricornutum* (*Pt*) account for up to 25% of all carbon fixation via photosynthesis.[2] The photosynthetic pigments of interest in light harvesting are noncovalently bound in the photosystems (PSs) and the light-harvesting complexes (LHCs) localized in the thylakoid membranes within the chloroplasts of these organisms. The thylakoids are organized in bands of three each (Figure 1a), which lack the grana-stroma differentiation typical for higher plant plastids, and the precise lateral distribution of the photosynthetic proteins therein is so far unknown.

Photosynthetic activity commences in the LHC, effectively the fucoxanthin chlorophyll *a*/*c* proteins (FCP) in diatoms,[3] which bind fucoxanthin (*Fx*), chlorophyll *a* (*Chl a*) and *c* (*Chl c*), as well as diadino- and diatoxanthin. The primary excitation target in our study, and principal light harvester, is *Fx*, the FCP-specific carotenoid whose absorption lies in the blue−green range (450−550 nm). *Fx*, along with *Chl c*, efficiently absorbs the solar energy that penetrates the water layer and transfers energy to the *Chl a*'s in the FCPs and then onto the reaction center (RC) of both photosystems, PSI and PSII, eventually to be stored as potential chemical energy. The two laser wavelengths used in this study, 473 and 532 nm, excite varying populations of energetically different *Fx*'s, as well as *Chl c* (Figure 1b), and on the basis of the images that map the emission from the terminal *Chl a* emitters localized in the FCPs and in the RCs of PSI and PSII, information about the spatial

Special Issue: Rienk van Grondelle Festschrift

Received: February 28, 2013
Revised: July 10, 2013
Published: July 11, 2013

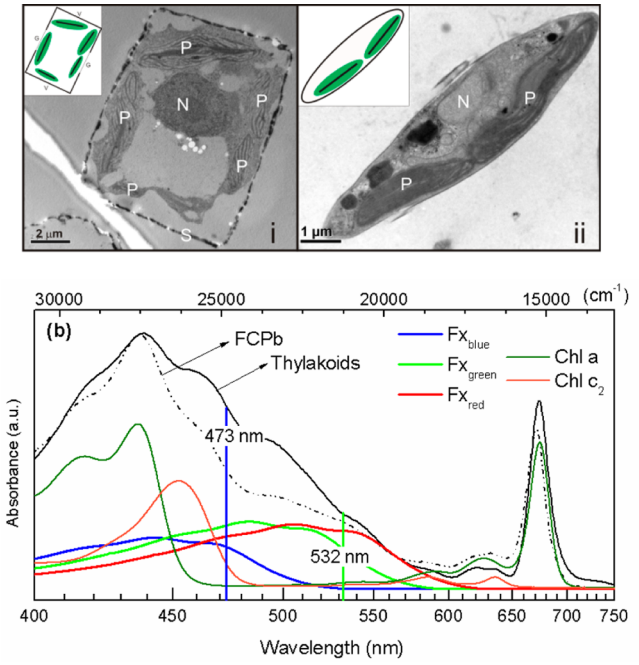

Figure 1. (a) Transmission electron micrograph (TEM) images of (i) *Cm* and (ii) *Pt* (UTex strain) cells: P, plastid; N, nucleus; S, silica shell; and in the left inset, G, girdle; V, valve, of the silica shell wall of *Cm*. Schematic representations of the cells with plastids (green) and the main direction of thylakoids within (black bars) are shown in the insets. (b) Absorptions of the FCPb complexes from *Cm* in dashed lines and the thylakoids (extracted from *PtUTex*) in solid lines. Also shown are the (scaled-up) component pigment spectra of *Fx* and *Chl*, which fit the FCP absorption (taken from ref 7) from which the relative amounts of pigments excited at 473 and 532 nm can be estimated.

distribution, and therefore the functional significance, of the primary absorbers may be inferred. Although examples of diatom images abound in microscopy,[4,5] the associated fluorescence spectra are not typically measured and have therefore not been studied in detail in terms of the electronic properties and spatial distribution of the emitting pigments, as we do here.

At the two excitation wavelengths used here, different populations of *Fx* are excited, with 473 nm exciting nearly equal amounts of all *Fx* molecules (i.e., Fx_{blue}, Fx_{green}, and Fx_{red}) and some *Chl c*, whereas 532 nm is preferentially absorbed by the lower-energy Fx_{red}, as well as Fx_{green} to a lesser extent (Figure 1b).[6,7] Fx_{red} and Fx_{green} have been shown to be highly efficient light harvesters,[8,9] with the former having notably large charge-transfer character,[6] whereas Fx_{blue} is proposed to be analogous to the LHCII luteins,[8] providing structural stability and photoprotection to the FCP complex besides functioning as a light harvester. Therefore, the differences in the *Chl a* emission should elucidate the links between the terminal emitters in the energy-transfer (ET) pathway and the excitation of the primary harvesters at 532 versus 473 nm. Thus, we may infer where Fx_{red} versus the other pigments, Fx_{blue}, Fx_{green}, and *Chl c*, are preferentially localized and active. Note that these emitting *Chl a*'s are primarily located in the antennae or PSII complexes with fluorescence from PSI typically having low yields in vivo at room temperature.[10]

Besides the spectroscopic properties associated with photosynthesis, diatoms have also garnered attention due to the properties associated with their silica shell microstructure and ability to manipulate light, for example, to be used as optical sensors, passive waveguides, diffraction elements for solar cells, photonic crystal lasers, and biomimetic applications.[11−13] Among the diatoms studied here, *Cm* has a distinct silica shell visible under the microscope, but neither of the two *Phaeodactylum* strains studied here possess this silica shell under the conditions in which they are grown. Depending on environmental conditions, the presence of the silica shell could have a profound effect on the nature and strength of the light that impacts the chloroplasts; these effects on the spectral signature of *Cm* are also discussed.

The current study explores the potential to characterize the spectral properties and responses of photosynthetic organisms in vivo and may serve as a basis for more detailed studies in the future to pinpoint and clarify our initial findings.

MATERIALS AND METHODS

Samples. *Cm* (Culture Collection Göttingen (SAG)) was grown in ASP medium according to Provasoli et al.,[14] supplemented with 2 mM silica. Two strains of *Pt*, UTEX strain 646 (*PtUTex*) and SAG strain 1090-1a (*Pt1a*), were cultured under the same conditions but without silica, and for the latter, the f/2 medium[15] was used.

The *Cm* and *PtUTex* diatoms shown in the transmission electron microscopy (TEM) images in Figure 1a were prepared and imaged according to Beer et al.[16]

Instrumentation and Measurement. Room-temperature (RT) absorbances of *Cm* FCPs, diatom thylakoids (both isolated as described in ref 17), and whole diatom cells were measured in a JASCO V550 absorption spectrometer. RT fluorescence spectra of *Cm* and *Pt* cells were measured in a JASCO (FP 6500) fluorimeter with 1 cm excitation and 0.5 cm emission path lengths and excitation/emission band-pass lengths set to 3 nm. Excitation and emission spectra were corrected using an R6G spectrum and a calibrated lamp spectrum, respectively. Concentration-dependent fluorescence spectra of *Pt1a* were measured for absorbances between 0.03 and 4.0 OD near the *Chl a* Q_y band maximum at 680 nm.

To image the diatoms, a 20−30 μL aliquot of each diatom colony in its medium is dropped onto a microscope slide onto which a thin glass coverslip is either taped down or glued with nail polish. The coverslip side of the cell "sandwich" is then placed on the microscope stage, facing the objective (40×) of an inverted microscope (IX70-71 Olympus). Emitted light passes through an adjustable pinhole and beam splitters (BFT-NIR-70-2501 or BFT-VIS-70-2501 (Melles Griot)) at 45° incidence. The emitted light is collected by a T64000 (Horiba-JY) spectrometer that employs a triple monochromator in a subtractive mode to minimize Rayleigh scattering and then projected onto a −70 °C Peltier cooled CCD (Andor).

The laser beams used to obtain the scanned images at 473 (Cobolt Blues, 25 mW) and 532 nm (Quantum optics, 500 mW) excitations were focused to a spot size of 1 × 1 μm on a selected diatom, always first exciting at 532 nm and then at 473 nm. Laser intensities were adjusted (always <1 mW at the objective focus) by verifying the reproducibility of a fluorescence spectrum at 1S integration. To prevent/minimize bleaching and undue stress and avoid physical drifting of the cell, integration times are kept to 0.25−1.0 s, which results in 30−45 min to obtain a complete scan. Under these constraints, about 5−10% of all sampled diatoms remain intact and survive the scans after both excitations. To image a single lateral slice,

dx.doi.org/10.1021/jp402094c | J. Phys. Chem. B 2013, 117, 11272−11281

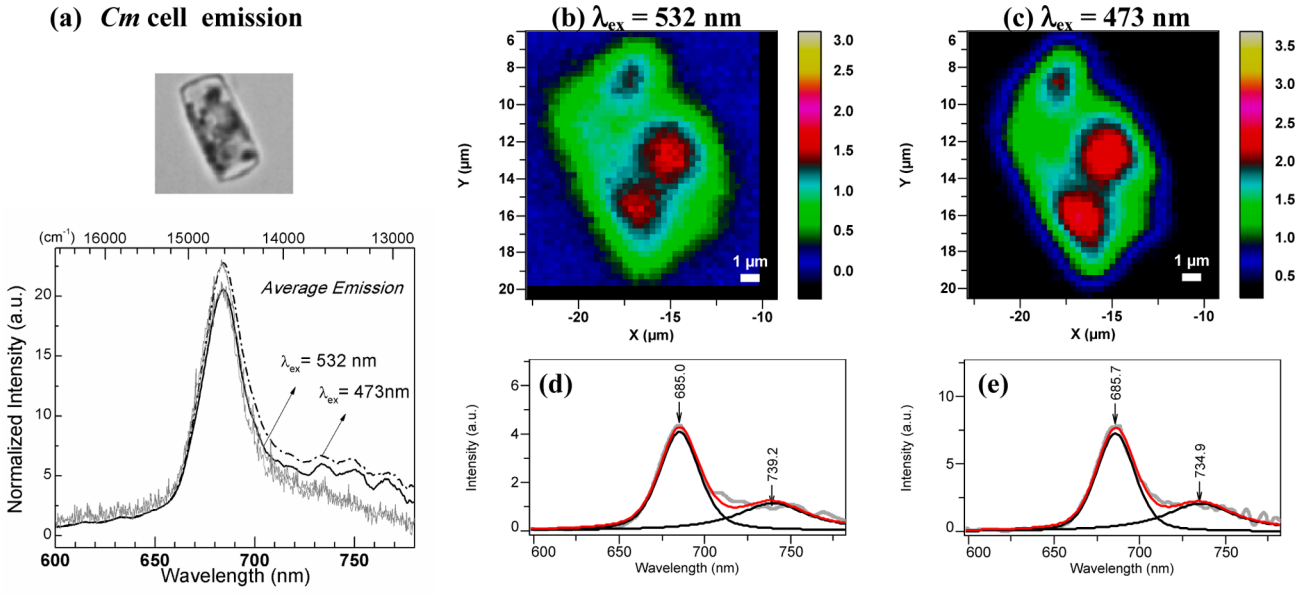

Figure 2. The fluorescence from a *Cm* cell measured at 532 (12 × 15 μm frame) and 473 nm (15 × 17 μm frame) excitations, with a pixel size of 0.3 × 0.3 μm. In (a), the fluorescence averaged over the whole image is shown for excitation at 532 (solid line) and 473 nm (dot−dash line) on a linear wavelength scale from 600 to 780 nm, with a low-resolution image (40× objective) of the diatom shown above. The images in (b) and (c) correspond to the total fluorescence intensity upon excitation at 532 and 473 nm, respectively (shown in the same size frame). Examples of the fit to the fluorescence from one pixel (x= −15.1, y = 12.1) of the images in (b) and (c) are shown in (d) and (e), respectively, where the fluorescence is shown in thick gray lines, the Gaussian bands in thin black lines, and the fit spectrum in red lines. (The component images to the fit, their co-localization, and the spread of the fit emission maxima, at 532 and 473 nm, are shown in Figure S1 in the Supporting Information.)

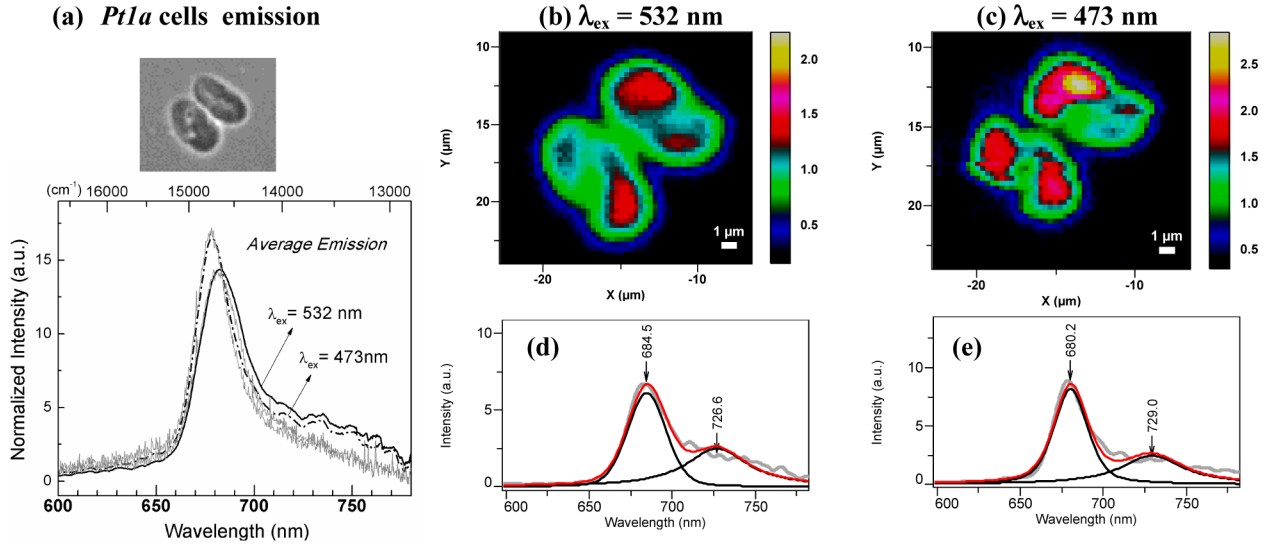

Figure 3. The fluorescence from two *Pt1a* cells measured at 532 and 473 nm excitations, in 18 × 14 μm sized frames with a pixel size of 0.4 × 0.4 μm. (a) Low-resolution image of the imaged *Pt1a* cells, with the fluorescence averaged over the whole image for excitation at 532 (solid line) and 473 nm (dot−dash line) from 600 to 780 nm (see Figure 2 for details). The images in (b) and (c) correspond to the total fluorescence intensity upon excitation at 532 and 473 nm, respectively (shown in the same size frame). Examples of the fit to the fluorescence from one pixel of the image in (b) at 532 nm (x= −14.4, y = 12.4) and in (c) at 473 nm (x= −14.2, y = 12.2) are shown in (d) and (e), respectively. The component images to the fit, their co-localization, and spread of the fit emission maxima, at 532 and 473 nm, are shown in Figure S1 (Supporting Information).

the smallest pixel is on the order of 0.3 × 0.3 μm for *Pt* and small *Cm* cells and 0.5 μm for larger *Cm* cells with slice thicknesses of ∼5 μm with the pinhole open. The objective is focused (typically 2−4 μm) to capture maximum fluorescence. Three examples, one each of *Cm*, *Pt1a*, and *PtUTex*, are shown in Figures 2−4. For the confocal images shown in Figures 5 (*Cm*) and 6 (*Pt1a*), the pinhole set at 0.7 or 1 μm leads to slice thicknesses of 0.58 and 0.83 μm, respectively, and are obtained at five or six depths, in 3 μm steps.

Image Analysis. The samples are rastered using a piezo stage, and full fluorescence spectra are obtained at every pixel of the image. Labspec5 (Horiba-JY) software is used to simultaneously fit 100s of fluorescence spectra from each image to two or three Gaussian−Lorenztian bands. A nonlinear peak-fitting routine, using a Levenberg−Marquardt algorithm, iteratively adjusts each parameter, the peak position, height, and full width at half-maximum (fwhm), to minimize χ^2. The initial values are set close to the best-fit values to the average

dx.doi.org/10.1021/jp402094c | J. Phys. Chem. B 2013, 117, 11272−11281

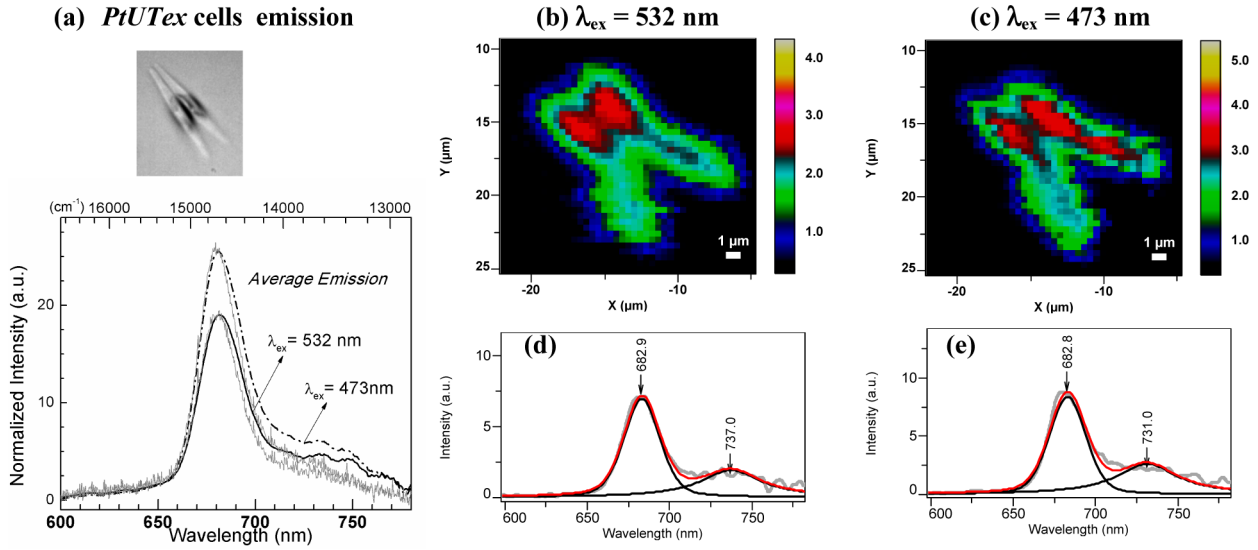

Figure 4. The fluorescence from two *PtUTex* cells measured at 532 and 473 nm excitations, in 18 × 16 μm sized frames with a pixel size of 0.4 × 0.4 μm. (a) Low-resolution image of the *PtUTex* cells and the fluorescence averaged over the whole image for excitation at 532 (solid line) and 473 nm (dot−dash line) from 600 to 780 nm (see Figure 2 for details). The images in (b) and (c) correspond to the total fluorescence intensity upon excitation at 532 and 473 nm, respectively (shown in the same size frame). Examples of the fit to the fluorescence from one pixel (x= −16.7, y = 14.5) of the images in (b) and (c) are shown in (d) and (e), respectively. The component images, their co-localization, and spread of the fit emission maxima, at 532 and 473 nm, are shown in Figure S1 (Supporting Information).

spectrum, and the peak values are constrained to 677−685 nm for the most intense band, and to 710−740 nm for the lower-energy band in the case of a two-band fit, and for a three-band fit, they are constrained between 700 and 715 nm for the middle band and 720 and 740 nm for the lowest-energy band. The heights are allowed to freely vary, whereas the fwhms are constrained to be <35 (for three bands) or <45 nm (for two bands).

All fluorescence spectra are corrected by the instrument response function, which has a noticeable effect above 700 nm (see corrected versus uncorrected spectra in Figures 2−4) and, despite the low S/N in this region, is crucial to obtain accurate fits to the fluorescence. The contrast and brightness of the (RGB) color images shown in Figures 2−6 are adjusted for best visualization. Co-localization plots (shown in the Supporting Information) were obtained in Fiji (Image J) by comparing the intensity spread between the deconvolved components at a given excitation wavelength. It was not possible to obtain co-localization plots between images excited at 532 versus 473 nm as the diatom (chloroplasts) invariably moved between scans.

RESULTS

Fluorescence Images of Diatoms Excited at 473 and 532 nm. The fluorescence imaged from lateral slices of *Cm*, *Pt1a*, and *PtUTex* cells are shown in Figures 2−4, respectively, in voxels of 3 μm × 3 μm × 5 μm. In panel (a), a low-resolution image of the diatom and the average emission over the scanned area, at 532 (solid line) and 473 nm (dash−dot line) excitations, is shown. The corresponding images are shown in (b) at λ_{exc} = 532 nm and in (c) at λ_{exc} = 473 nm, with examples of the fit to the fluorescence from one pixel shown in (d) and (e), respectively. Two Gaussians, modeling the main Q_y band at ∼682 nm and the lower-energy band at ∼730 nm, suffice to produce good fits to the spectra of diatoms that remain intact after scanning, aside from a small minority of pixels where a shoulder at ∼710 nm is evident between the modeled bands. The component images from these fits are shown in Figure S1a (Supporting Information). Co-localization threshold calculations show that the two (fit) bands are mostly co-localized (Figure S1b, Supporting Information), but these calculations are however prone to error where the signal intensity is low, that is, at the chloroplast edges where there is some suggestion that either the 680 nm band (*Pt1a*) or the low-energy band (*PtUTex*) could dominate (Figure S1a, Supporting Information). Overall, the two-band fit confirms that the low-energy emission primarily arises from the vibronic sideband of the Q_y transition of *Chl a*.

Useful information about the spatially related spectral response of the *Chl*'s can also be obtained by plotting the spread of the emission maxima from the Gaussian fits at 532 versus 473 nm excitations (Figure S1c, Supporting Information); in *Pt1a*, the Q_y band maxima upon 532 nm excitation are much redder than those at 473 nm, whereas this difference is not so obvious for the main Q_y band in *Cm* and *PtUTex*. In contrast, the lower-energy band, while noisy, is more consistently to the red upon 532 nm excitation in all species. The average emission maxima (Table 1) also reflect this trend, being similar at both excitations for *Cm* (∼684 nm) and *PtUTex* (∼679 nm), whereas *Pt1a* emission upon 532 nm excitation (∼683 nm) is about 2 nm redder than that at 473

Table 1. Fluorescence Properties of Individual Diatoms

	λ_{em}^{max} from (C)LSF images[a]	
sample[a]	λ_{exc} = 473 nm[b]	λ_{exc} = 532 nm[b]
Cm	682−686 (684.4 ± 1.4)	682−686 (684.9 ± 1.5)
Pt1a	678−682 (680.1 ± 1.3)	680−682 (682.9 ± 1.9)
PtUTex	678−681 (678.6 ± 1.3)	679−681 (679.9 ± 0.8)

[a]The spread in the fluorescence emission maxima, with the mean and standard deviation in parentheses, of intact diatoms obtained from five independent (C)LSF measurements are listed for *Cm*, *Pt1a*, and *PtUTex*. [b]At 473 and 532 nm excitations. (Note that the 710 nm band is not evident in any of the emission spectra for the results above.)

dx.doi.org/10.1021/jp402094c | J. Phys. Chem. B 2013, 117, 11272−11281

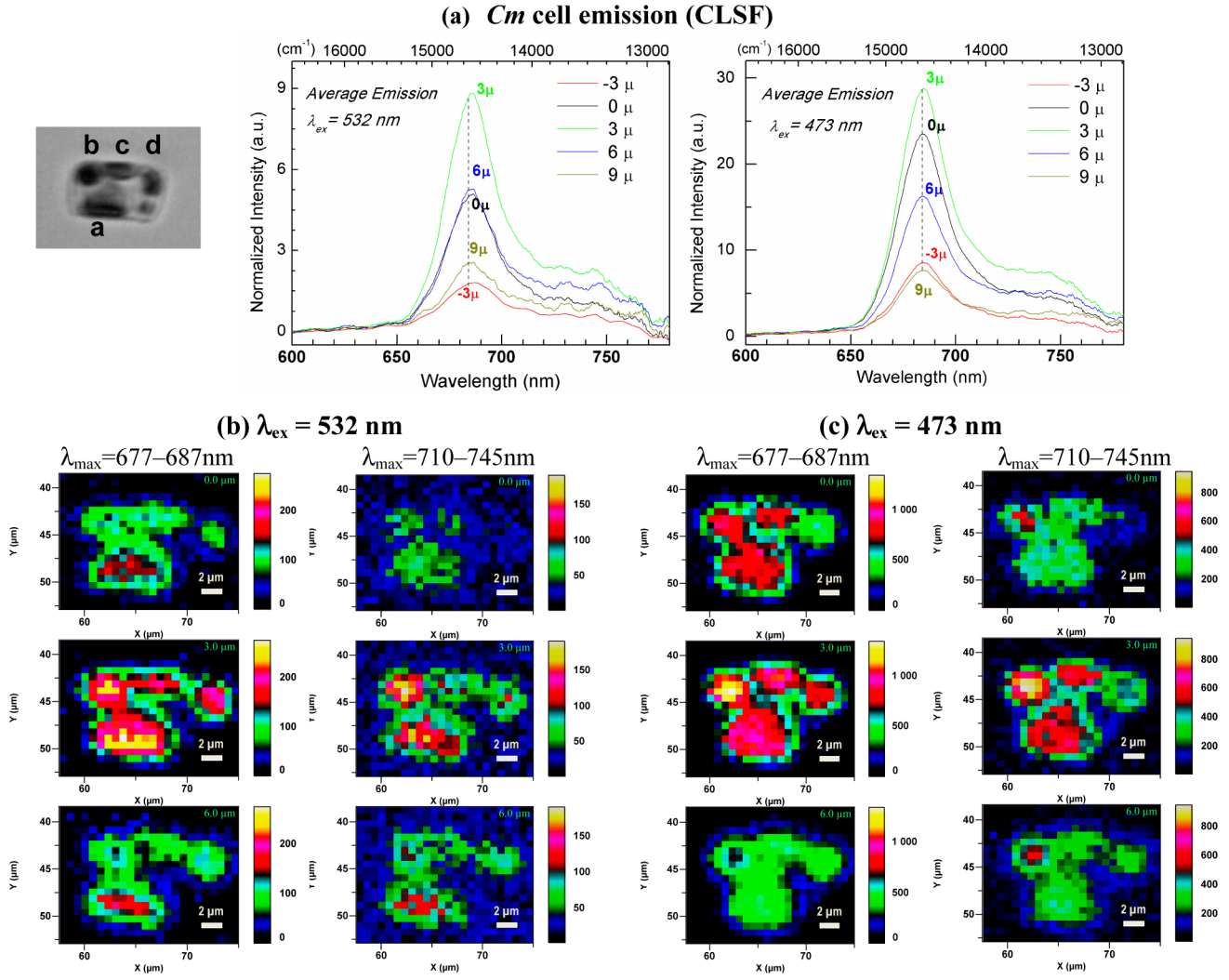

Figure 5. The fluorescence measured from the CLSF scans of a *Cm* cell. (a) Low-resolution image of the *Cm* cell with the five chloroplasts therein labeled from "a" to "d", along with the five fluorescence spectra measured at −3 (red), 0 (black), +3 (green), +6 (blue), and +9 μm (brown), from 600 to 780 nm, at 532 (left) and 473 nm (right) excitations (the vertical line is at 684 nm). The components deconvolved from the total fluorescence (λ_{max} fit between 677 and 687 nm on the left and λ_{max} fit between 710 and 745 nm on the right) are shown at 0, +3, and +6 μm depths, consecutively one below the other, at 532 nm excitation in (b) and at 473 nm excitation in (c). All images are obtained in 20 × 15 μm frames composed of 0.7 × 0.7 × 0.8 μm voxels. (The spread of the fit emission maxima and the average fluorescence from each chloroplast at each depth, at 532 and 473 nm excitations, are shown in Figure S3 in the Supporting Information.)

nm. Overall, *Cm* tends to emit more to the red than *Pt* cells, and *PtUTex* has the bluest emission at both 473 and 532 nm excitation. (In addition, we note that when cells are broken, midscan, or otherwise, the fluorescence maximum blue shifts to between 675 and 678 nm for all three diatoms, with further enhancement of emission upon 473 nm excitation.)

Aside from these examples shown for fluorescence typically imaged from these diatoms, a band at ∼710 nm is also sometimes evident in the average fluorescence spectrum of *Pt1a* cells from young cultures, an example of which is shown in Figure S2 (Supporting Information), and seen in the confocal image of *Pt1a* (discussed below). We note that this 710 nm band is detected in less than 10% of the *PT1a* cells scanned from cultures in the exponential growth phase, whereas up to 50% of *Pt1a* cells exhibit the 710 nm emission 5−7 days later. In *PtUTex*, the band appeared only after 1−2 weeks, and in *Cm*, it appeared at even later times, all toward the beginning of the stationary growth phase.

Confocal Images of *Cm* and *Pt1a* Excited at 473 and 532 nm. The confocal fluorescence images of *Cm* (Figure 5) and *Pt1a* (Figure 6) cells, measured in 3 μm increments, provide additional information about the pigment distribution as a function of depth within the diatom chloroplasts.

The *Cm* diatom shown in Figure 5, at 0, 3, and 6 μm depths, is on its side and has four chloroplasts labeled a−d (inset of Figure 5a). A crude evaluation of the average emission from each chloroplast (Figures 5 and S3 (Supporting Information)) indicates that the emission varies heterogeneously as a function of depth and that the distribution of the *Chl a*'s that accept energy from the 532 nm absorbers, the Fx_{red}'s as well as the Fx_{green}'s, differs from the distribution of those that accept energy from the 473 nm absorbers. Furthermore, the ratio of emission upon 473 versus 532 nm excitation becomes higher toward the interior in most chloroplasts (the table in Figure S3, Supporting Information), implying that pigments absorbing at 532 nm are more abundant toward the edges of the chloroplasts. Second, although the emission density from

dx.doi.org/10.1021/jp402094c | J. Phys. Chem. B 2013, 117, 11272−11281

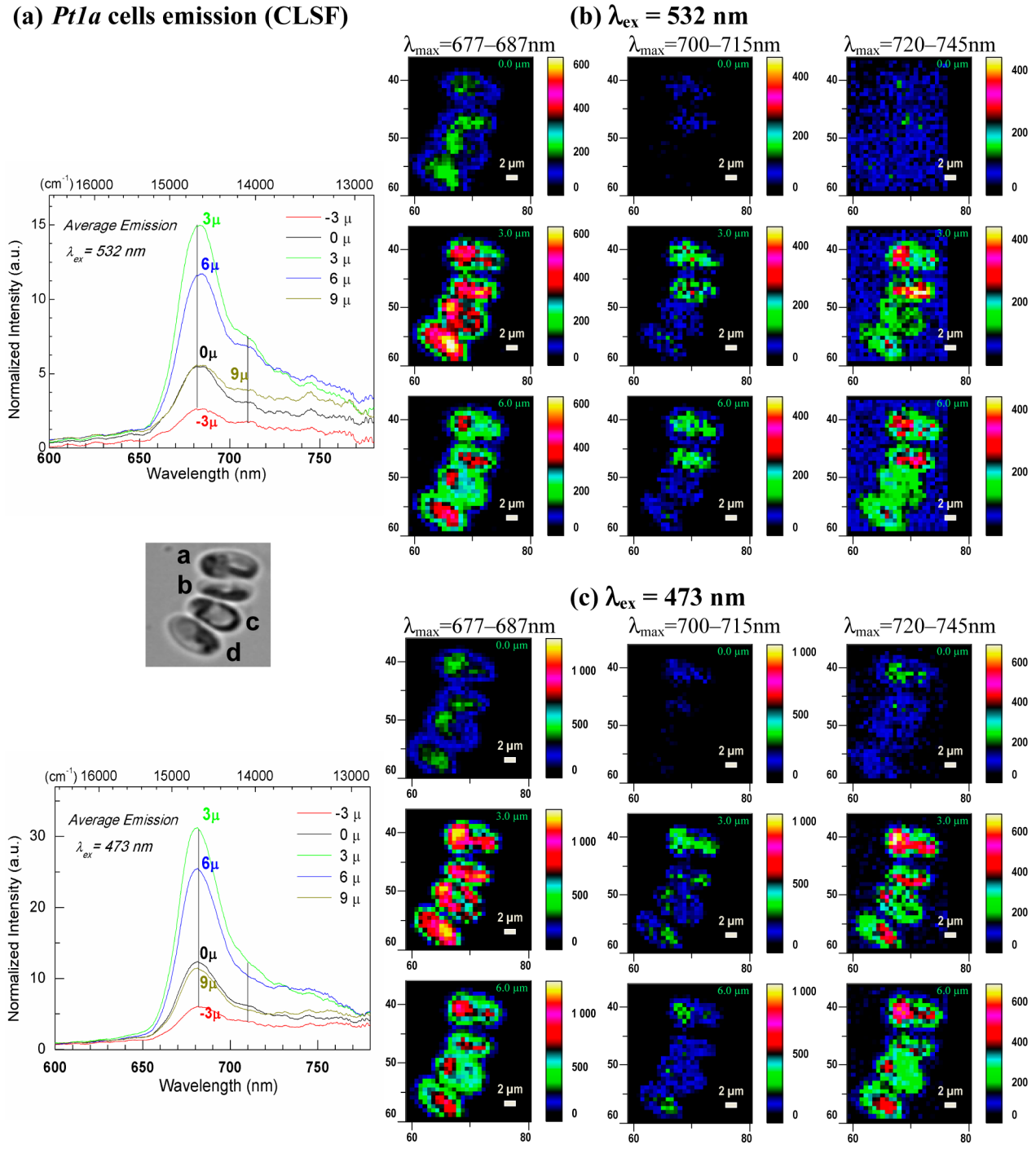

Figure 6. CLSF images and fluorescence spectra of a four *Pt1a* cells. (a) Low-resolution image of the four *Pt1a* cells, labeled a–d, and the fluorescence, averaged over the whole image from all four cells, shown for 532 (above) and 473 nm (below) excitations, measured at −3 (red), 0 (black), +3 (green), +6 (blue), and +9 μm (brown), from 620 to 780 nm (the vertical lines are at 680 and 710 nm). The images corresponding to the three components deconvolved from the total fluorescence (λ_{max} fit between 677 and 685 nm (left), 700 and 715 nm (middle), and 720 and 745 nm (right)) are shown at 0, +3, and +6 μm depths, consecutively one below the other, at 532 nm excitation in (b) and at 473 nm excitation in (c). All images are obtained in 22 × 22 μm frames composed of 1.0 × 1.0 × 0.8 μm voxels, with the *x*-axis horizontal and the *y*-axis vertical. (The spread of the fit emission maxima, the average fluorescence from each cell at each depth at 532 and 473 nm, and the co-localization maps at 532 nm are shown in Figure S4 of the Supporting Information.)

exciting a much greater number of pigments at 473 nm is much higher, it is clear that the terminal *Chl a* emitters that accept energy from the 532 nm absorbing *Fx*'s are just as widespread as the former (Figures 5 and S3 (Supporting Information)).

The plot of the spread in the peak emission maxima shows that 532 nm excitation here too results in redder emission than that at 473 nm, particularly in chloroplast a (see yellow pixels in Figure S3a, Supporting Information), and points to a different set of emitting *Chl a*'s that accept energy from the non-Fx_{red} light harvesters at 473 nm to the Fx_{red} absorbers at 532 nm. At 532 nm excitation, the redder emission maxima are accompanied by a small blue shift in the average emission

dx.doi.org/10.1021/jp402094c | J. Phys. Chem. B 2013, 117, 11272–11281

maximum from −3 to +3 μm, which then red shifts back again at greater depths (see the table in Figure S3, Supporting Information), again pointing to different sets of final *Chl a* emitters that vary with depth, with apparently more red emitters at the edge of the plastids. The blue shift of the emission maximum with increasing depth moreover indicates that what we observe is not due to reabsorption or else it would lead to a red shift.

In contrast to *Cm*, *Pt1a* cells typically contain only one or two plastids, and the lobular shape of this plastid, which tends to be flattened and wrapped up along the cell wall in the *z*-direction, would affect the pigment density and distribution differently than that in *Cm*. This can be seen in the four chloroplasts labeled a−d of the *Pt1a* cells in Figure 6. Here, the clear presence of the red shoulder at ∼710 nm in the average fluorescence spectra (Figure 6a) required the total fluorescence be fit to three Gaussians. The component images from the fit, are shown at 0, 3, and 6 μm depths in (b) at 532 nm and in (c) at 473 nm excitation. The 710 nm fluorescence is much greater in cells a and b and co-localized with the main Q_y band (Figure S4c), similar to that in the *Pt1a* cells shown in Figure S2 (Supporting Information), but which also exhibit relatively greater emission upon 532 nm excitation.

Heterogeneous emission is also evident in that the *Pt1a* cell that emits maximally upon excitation at 532 nm is not necessarily the same maximum intensity emitter at 473 nm excitation; at 3 and 6 μm, cells a, c, and d appear to be equally strong emitters at 532 nm, whereas at 473 nm, a is the strongest emitter (see Figure S4, Supporting Information). The spread of the emission maxima from the fit to the Gaussian bands shows redder emission for all three components at 532 versus 473 nm excitation (Figure S4a, Supporting Information). This is also reflected in the average fluorescence maxima being slightly blue-shifted at all five depths upon excitation at 473 nm relative to that at 532 nm, although, unlike the *Cm* cell in Figure 5, there is no noticeable blue shift with increasing scanning depth, probably in part because of the greater 710 nm emission from two of the four *PT1a* cells.

Autofluorescence of Diatom Solutions. The low-concentration fluorescence spectra[18] of 1 mL solutions of *Cm*, *Pt1a*, and *PtUTex* cells (Figure 7a) show that the emission maximum of all three is centered at 683.0 ± 0.5 nm (Table 2). The emission intensity upon excitation at 532 nm is similar to that at 473 nm for *Cm* cells but about a third lower in *Pt* cells. At high cell concentrations, emission at longer wavelengths is enhanced due to re-absorption, and the main emission maxima are shifted to the red (Figure 7b). In addition, a 710 nm band is present, particularly in *Pt1a*, even at an OD as low as 0.04 (not shown) but also in *Cm* and *PtUTex*. In contrast to the single-cell spectra, the 710 nm emission band is just as dominant for excitation at 473 nm and is accompanied by a progressive red shift of the main fluorescence band to ∼690 nm (Figure 7b). This is a clear signature for the re-absorption of emitted photons in the solution spectra, in sharp contrast to the spectral features in single cells.

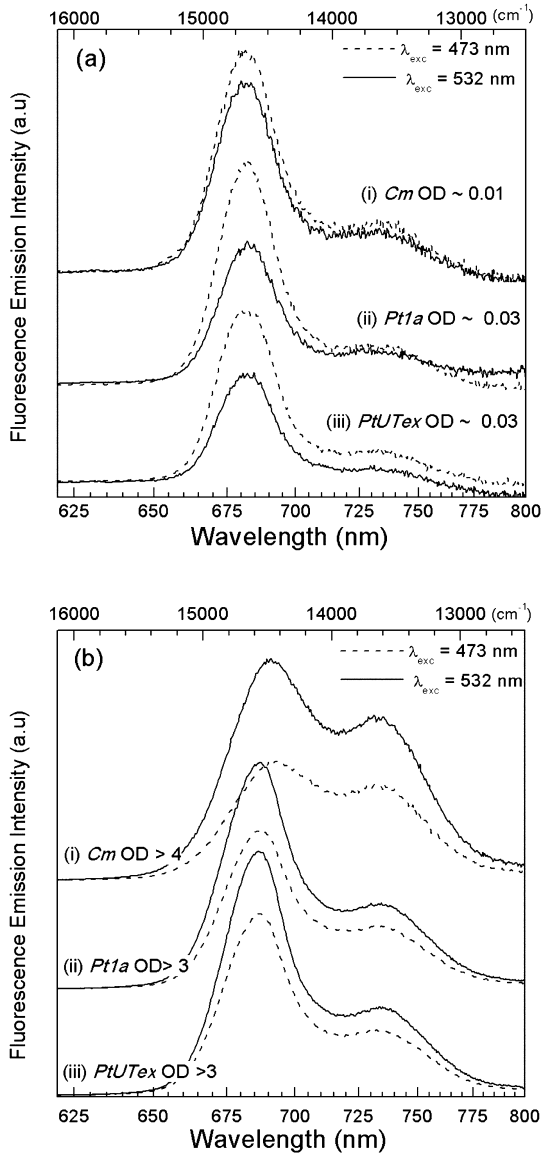

Figure 7. The fluorescence emission spectra of (i) *Cm*, (ii) *Pt1a*, and (iii) *PtUTex* cell solutions/suspensions are shown in (a) at low concentration (OD < 0.03 at 680 nm) and in (b) at high concentrations (OD > 3 OD at 680 nm). Emission spectra are measured at 473 (dashed line) and 532 nm (solid line) in a 0.5 cm path length cuvette. Note that all cells are from young cultures in the early growth stage.

DISCUSSION

One of the main objectives of the current exploratory study was to understand the effects on the fluorescence emission from live diatoms upon selectively exciting functionally different *Fx* molecules; using 532 nm primarily excites the red absorbers, two-thirds of which are Fx_{red}'s and the rest being Fx_{green}'s, and 473 nm excites about equal amounts of Fx_{blue}'s, Fx_{green}'s, and Fx_{red}'s, as well as some *Chl c* (Figure 1b).[6] These pigments are bound in the FCP complexes, and the measured emission at RT primarily arises from terminal *Chl a* emitters that are bound in the FCPs and in the PSII complexes, all within the thylakoids localized in the chloroplasts of the diatoms. The total fluorescence yield and the ratio between FCP and PSII fluorescence in a living cell further depend on regulation phenomena, for example, due to the reduction state of PSII and protective mechanisms like nonphotochemical quenching. Although the resolution of the measured (C)LSF images (at best 300 nm) does not allow us to differentiate between fluorescence arising from the FCPs versus that from PSII, the spatial variation in the intensity and energy of the fluorescence provides useful information about the spectral response at a subcellular level. Complementarily, solution spectra measure

dx.doi.org/10.1021/jp402094c | J. Phys. Chem. B 2013, 117, 11272−11281

Table 2. Fluorescence Properties of Low-Concentration Diatoms in Solution

sample[a]	λ_{em}^{max}[a] λ_{exc}^{473}	λ_{exc}^{532}	excitation ratio[b]	emission ratio[c]
Cm	682.0	682.5	0.90−1.0	0.86−1.00
Pt1a	683.0	683.5	0.66 − 0.75	0.62−0.74
PtUTex	682.5	682.5	0.71	0.62−0.69
thylakoids	680.0	679.5		0.66

[a]The fluorescence emission maxima are from low-concentration (<0.03 OD) solutions of diatoms using the same two excitation wavelengths as those used in the CLSF experiments, 473 and 532 nm (see Table 1), for *Cm*, *Pt1a*, and *PtUTex*, as well as thylakoids extracted from *PtUTex* cells. [b]The ratio of the fluorescence intensities at 532 versus 473 nm for the emission collected near the maximum at ∼681 nm (Figure S5, Supporting Information). [c]The ratio of the intensities at the emission maxium at ∼681 nm upon excitation at 532 versus 473 nm (Figure 7a).

the ensemble spectral response of the diatoms and allow a comparative analysis of the spectral response from single cells.

Spatial Organization of the Spectrally Different Diatom Pigments. When comparing the diatom fluorescence in low-concentration solutions to that of single cells, the λ_{ems} maxima are consistent under both conditions (Tables 1 and 2). The single-cell spectra however exhibit a larger variability/range in emission maxima and in the relative amount of fluorescence (yields) upon excitation at 532 versus 473 nm, which is most evident in the confocal images at different depths (Figures 5 and 6). This could result from the way in which the excitation source "samples" the chloroplast and the associated pigment distribution: in solution, pigments at the surface of the cells would be preferentially excited by the photons from the fluorimeter's broad-beam lamp, whereas pigments deeper within the chloroplast would be accessible to photons from the laser beam that penetrates more deeply (in the *z*-direction), albeit attenuated on its way through the chloroplast.

In this regard, the apparent loss in relative emission upon excitation at 473 versus 532 nm with increasing depth in the *Cm* cell in Figure 5 (also see the table in Figure S3, Supporting Information) argues for increased shading, an effect that could be more pronounced in the bean-shaped chloroplasts of *Cm* compared to the flatter *Pt* plastids (Figure 1a). Notably, there is also a difference in the ratio of emission at the two different excitation wavelengths that appears to be species-dependent; in solution, both *Pt* diatoms exhibit lower emission at 532 versus 473 nm excitation (Figure 7a), whereas the emission from *Cm* diatoms is almost the same at both wavelengths and could arise from a combination of the following: (a) emission upon 473 nm excitation is more efficiently re-absorbed in *Cm* potentially because of the presence of multiple chloroplasts, (b) differences in the abundance of the complexes that bind redder versus bluer absorbing *Fx*'s, and (c) differences in the amounts of the accessory pigments. Interestingly, different FCP complexes in both *Cm* and *Pt* have been shown to bind varying amounts of more blue- versus more red-absorbing *Fx* molecules while having equal amounts of *Chl c*.[17,19] In addition, it was shown that a greater amount of Fx_{red} is connected to PSII, whereas PSI receives relatively more energy from the Fx_{blue}'s and Fx_{green}'s.[20,21]

Differential binding of Fx_{red} is also implied in the CLSF images of the *Cm* cell wherein the ratio of emission at 473 versus 532 nm excitation increases toward the middle of the plastids, pointing to more Fx_{red}'s localized toward the edges of the plastids. On the basis of the differential *Fx* binding[19] and the link to PSI and PSII[20,21] this points to the presence of PSII complexes, and FCPs binding greater amounts of Fx_{red}'s at the periphery of the chloroplasts. In addition, the small blue shift deeper within the cell, upon excitation at 532 nm in the *Cm* cell (Figure S3, Supporting Information), could reflect a higher number of proteins containing bluer fluorescing pigments localized deeper within the chloroplast of these organisms. Because FCPs emit at higher energies in comparison to PSII and the very low fluorescing PSI complexes at RT, this suggests an overall enrichment of FCPs in the interior of the chloroplasts. Note that this spatial separation is only obvious in *Cm* cells. On the other hand, *Pta1* shows a much stronger distinction in the sets of *Chl a*'s receiving energy from the various 473 nm absorbers versus the Fx_{red}'s at 532 nm; the bluer emission in the former case indicates greater fluorescence from FCP at 473 nm, compared to that from PSII upon excitation at 532 nm.

Despite targeting fewer pigments, the wide lateral spread of the 532 nm induced emission indicates that red-edge excitation ensures effective ET no matter which part of the chloroplast is exposed to the incident light. The advantage of this lateral spread in Fx_{red}-containing complexes may be inferred from the high-concentration solution spectra that indicate that the Fx_{red}'s are extremely efficient at being able to absorb the residual light for light harvesting and ET, as evidenced by almost the same fluorescence yield despite its lower absorption in comparison to the bluer-absorbing pigments. It may therefore be argued that the Fx_{red}'s would more efficiently compensate for the quenching associated with tight intracellular pigment packing if the complexes in which they are bound are (more) widely distributed within the organelle.

Anomalous Emission Properties at the Red Edge (710 nm band). Although observed in less than 10% of *Pt1a* cells imaged from fresh cultures, the significance of the 710 nm has been noted and observed at RT in *Pt* cells grown under red light.[22] In diatom solutions, we observe the 710 nm band only at high concentrations, that is, when re-absorption apparently increases its yield. Thus, it is accompanied by a noticeable red shift of the emission band and relatively lower emission upon bluer excitation at 473 versus 532 nm (Figure 7b).

A contrasting picture emerges upon examining the results from the fluorescence spectra of single cells that exhibit noticeable 710 nm emission. The main fluorescence band of single *Pt1a* cells does not obviously red shift, and more importantly, the 710 nm band is weak or almost absent upon excitation at 473 nm (Figures S2 (Supporting Information) and 6). In terms of pigment distribution, the predominant 532 nm response should therefore be linked to the FCPs binding more of Fx_{red}, the only complex that absorbs at this wavelength, and the change in emission could thus arise either from the organization of the FCPs themselves, for example, due to enhanced aggregation, or from FCPs that are biochemically yet uncharacterized due to their low abundance in thriving cultures. We note that the 710 nm emission in *Pt1a* is much more evident in older cultures both in single cells and in solution (Figure S5, Supporting Information), but the emission maximum is unchanged unlike the case in high-concentration solutions, again mainly present upon 532 nm excitation, and therefore should have a different origin than re-absorption. Thus, the 710 nm emission also appears to be generally related to a stress response, whereby the aged *Pt1a* cultures could be

dx.doi.org/10.1021/jp402094c | J. Phys. Chem. B 2013, 117, 11272−11281

"stressed" due to environmental factors like high cell density, light intensity, or nutrient depletion.[23,24]

Role of the Silica Shell in Light Harvesting and Photoprotection. Among the three diatom species studied, *Cm* is the only one that possesses a sturdy silica shell, whereas the *Pt* species are both grown in the absence of silica and could account for differences in their excitation-wavelength-dependent emission intensities, variation in pigment densities along the length of the chloroplasts (*Cm* in Figure 5 versus *Pt* in Figure 6), and the presence of the 710 nm emission, which in *Cm* is manifested only much later in the growth phase than that in *Pt1a*. If the latter can partly be attributed to an age- or environment-related stress response, *Cm* could potentially be considered a more robust species. If it is the silica shell that confers this hardiness, then it must work beyond being a physical shield and somehow also influence photosynthetic activity in the organism.

One such influence could arise from the well-known waveguide properties of the silica shell that is shown to enhance the intensity of the absorbed light and more specifically the coupling of blue−green light with the girdle versus red light with the valve (Figure 1a).[11] In this case, depending on environmental conditions, chloroplasts in *Cm* could move away from the cell wall to protect themselves, for example, under high light intensity,[25] or alternatively, under low-light conditions, they could move closer to the silica shell wall to exploit the enhanced light.

An interesting effect of being close to the evanescent field near the silica shell[11] is that it could enhance the known charge-transfer properties and the concomitant light harvesting of the Fx_{red}'s (and Fx_{green}'s)[6] via an enhancement of the potential difference between the membrane and silica shell. This could partly explain the relatively higher emission at 532:473 nm excitations in *Cm* versus *Pt* cells, which is ∼1:1 in the former and 0.7:1 in the latter (Table 2). These adaptive mechanisms in the silica-shell-containing *Cm* diatoms would need to be suitably modified in the absence of the silica shell in the *Pt* cells. Therefore, it is possible that in the case of a close approach of adjacent *Pt* cells, intercellular effects could be provoked more easily, such as, for example, shading.

CONCLUSIONS

The fluorescence spectra from the (C)LSF images of the *Cm*, *Pt1a*, and *PtUTex* cells show that the spatial distribution of emission is heterogeneous, on a 0.3−0.5 μm scale, and that there are differences in the spread of the emission maxima and intensity upon excitation at 473 nm versus 532 nm. The latter, which primarily excites Fx_{red}'s, results in emission from *Chl a*'s that are just as, or more, widely distributed as the *Chl a*'s that accept energy from the more numerous pigments excited at 473 nm. Absorption of redder photons at 532 nm, in *Cm*, is attributed to FCP complexes containing relatively higher amounts of Fx_{red} that transfer their energy predominantly to PSII. Second, the variation in the relative fluorescence intensity at different depths in the chloroplast, at 532 versus 473 nm excitations, points to varying pigment (Chl and Cars) density, with more FCPs fluorescing at a shorter wavelength in the center of the plastids and preferential localization of Fx_{red}-enriched complexes at the periphery. Third, in *Pt1a*, the excitation at 473 nm leads to energy transfer to *Chl a*'s emitting at shorter wavelength as compared to excitation of predominantly Fx_{red} at 532 nm. In addition, in some single cells of *Pt1a*, a 710 nm band is prominent, which is not accompanied by a noticeable red shift of the main emission as in solution; and moreover is most evident upon excitation at 532 nm and can thus be attributed to the specific excitation, and potentially higher concentration, of FCP complexes containing more Fx_{red}. The single-cell spectra also demonstrate that there is a species-specific response, with *Pt1a* most readily emitting at 710 nm, an effect that is also dependent on the age of the cultures.

ASSOCIATED CONTENT

Supporting Information

Figure S1: The co-localization maps and the spread of the emission maxima for the deconvolved components of the fit to the total fluorescence for the diatoms in Figures 2−4. Figure S2: An example of a single lateral section of *Pt1a* cells that exhibit anomalous 710 nm emission. Figures S3 and S4: The spread of the emission maxima from the fit to the total fluorescence and the emission arising from the individual chloroplasts of the *Cm* and *Pt1a* cells in Figures 5 and 6, respectively. Figure S5: the fluorescence excitation spectra for low- and high-concentration diatom solutions and fluorescence spectra of older *Cm* and *Pt1a* cells in solution in the late growth phase. This material is available free of charge via the Internet at http://pubs.acs.org.

AUTHOR INFORMATION

Corresponding Author

*E-mail: premvard@gmail.com. Tel: +33-(0)6-14-94-63-82 (L.P.); E-mail: C.Buechel@bio.uni-frankfurt.de. Tel: +49-69-798-29602 (C.B.).

Notes

The authors declare no competing financial interest.

ACKNOWLEDGMENTS

L.P. and M.R. acknowledge Région Centre (France) for support. C.B. gratefully acknowledges support from the Deutsche Forschungsgemeinschaft (Bu812/4-1 and 4-2) as well as from the EU (MC ITN 238017 'Harvest'). L.P. would also like to acknowledge the rewarding scientific experience to challenge and learn during the time spent in the lab of R.v.G. and the fruitful collaborations, especially the one with C.B., that grew from this period.

REFERENCES

(1) Simon, N.; Cras, A.-L.; Foulon, E.; Lemée, R. Diversity and Evolution of Marine Phytoplankton. *C.R. Biol.* **2009**, *332*, 159−170.

(2) Field, C. B.; Behrenfeld, M. J.; Randerson, J. T.; Falkowski, P. G. Primary Production of the Biosphere: Integrating Terrestrial and Oceanic Components. *Science* **1998**, *281*, 237−240.

(3) Mimuro, M.; Katoh, T.; Kawai, H. Spatial Arrangement of Pigments and Their Interaction in the Fucoxanthin-Chlorophyll a/c Protein Assembly (FCPA) Isolated from the Brown Alga *Dictyota Dichotoma*. Analysis by Means of Polarized Spectroscopy. *Biochim. Biophys. Acta* **1990**, *1015*, 450−456.

(4) Shihira-Ishikawa, I.; Nakamura, T.; Higashi, S.-i.; Watanabe, M. Distinct Responses of Chloroplasts to Blue and Green Laser Microbeam Irradiations in the Centric Diatom *Pleurosira Laevis*. *Photochem. Photobiol.* **2007**, *83*, 1101−1109.

(5) Tang, Y. Z.; Dobbs, F. C. Green Autofluorescence in Dinoflagellates, Diatoms and Other Microalgae and Its Implications for Vital Staining and Morphological Studies. *Appl. Environ. Microbiol.* **2007**, *73*, 2306−2313.

(6) Premvardhan, L.; Sandberg, D. J.; Fey, H.; Birge, R. R.; Büchel, C.; van Grondelle, R. The Charge-Transfer. Properties of the S_2 State of Fucoxanthin in Solution and in Fucoxanthin Chlorophyll-a/c_2

Protein (FCP) Based on Stark Spectroscopy and Molecular-Orbital Theory. *J. Phys. Chem. B* **2008**, *112*, 11838−11853.
(7) Premvardhan, L.; Bordes, L.; Beer, A.; Büchel, C.; Robert, B. Carotenoid Structures and Environment in Trimeric and Oligomeric Fucoxanthin Chlorophyll-a/c_2 Proteins (FCP) from Resonance Raman Spectroscopy. *J. Phys. Chem. B* **2009**, *113*, 12565−12574.
(8) Papagiannakis, E.; van Stokkum, I. H. M.; Fey, H.; Büchel, C.; van Grondelle, R. Spectroscopic Characterization of the Excitation Energy Transfer in the Fucoxanthin-Chlorophyll Protein of Diatoms. *Photosynth. Res.* **2005**, *86*, 241−250.
(9) Gildenhoff, N.; Amarie, S.; Gunderman, K.; Beer, A.; Büchel, C.; Wachtveitl, J. Oligomerization and Pigmentation Dependent Excitation Energy Transfer in Fucoxanthin-Chlorophyll Proteins. *Biochim. Biophys. Acta, Bioenerg.* **2010**, *1797*, 1647−1656.
(10) Krause, G. H.; Weis, E. Chlorophyll Fluorescence and Photosynthesis: The Basics. *Annu. Rev. Plant Phys.* **1991**, *42*, 313−349.
(11) Fuhrmann, T.; Landwehr, S.; El Rharbi-Kucki, M.; Sumper, M. Diatoms as Living Photonic Crystals. *Appl. Phys. B: Laser Opt.* **2004**, *78*, 257−260.
(12) De Stefano, L.; Rendina, I.; De Stefano, M.; Bismuto, A.; Maddalena, P. Marine Diatoms as Optical Chemical Sensors. *Appl. Phys. Lett.* **2005**, *87*, 233902.
(13) Noyes, J.; Sumper, M.; Vukusic, P. Light Manupulation in a Marine Diatom. *J. Mater. Res.* **2008**, *23*, 3229−3235.
(14) Provasoli, L.; McLaughlin, J. J. A.; Droop, M. R. The Development of Artificial Media for Marine Algae. *Arch. Microbiol.* **1957**, *25*, 392−428.
(15) Guillard, R. R. L. Culture of Phytoplankton for Feeding Marine Invertebrates. In *Culture of Marine Invertebrate Animals*; Smith, W. L., Chanley, M. H., Eds.; Springer US, 1975; pp 29−60.
(16) Beer, A.; Juhas, M.; Büchel, C. Influence of Different Light Intensities and Different Iron Nutrition on the Photosynthetic Apparatus in the Diatom *Cyclotella Meneghiniana* (Bacillariophyceae). *J. Phycol.* **2011**, *47*, 1266−1273.
(17) Beer, A.; Gundermann, K.; Beckmann, J.; Büchel, C. Subunit Composition and Pigmentation of Fucoxanthin-Chlorophyll Proteins in Diatoms: Evidence for a Subunit Involved in Diadinoxanthin and Diatoxanthin Binding. *Biochemistry* **2006**, *45*, 13046−13053.
(18) The emission spectra of *Cm* and *Pt* cells recorded at the lowest concentrations (<0.03 OD) are closest to "true" emission spectra having minimized re-absorption, and with the emission intensities being linearly proportional to the excitation intensities (Table 2).
(19) Gundermann, K.; Büchel, C. Factors Determining the Fluorescence Yield of Fucoxanthin-Chlorophyll Complexes (FCP) Involved in Non-Photochemical Quenching in Diatoms. *Biophys. Biochim. Acta, Bioenerg.* **2012**, *1817*, 1044−1052.
(20) Szabó, M.; Premvardhan, L.; Lepetit, B.; Goss, R.; Wilhelm, C.; Garab, G. Functional Heterogeneity of the Fucoxanthins and Fucoxanthin-Chlorophyll Proteins in Diatom Cells Revealed by Their Electrochromic Response and Fluorescence and Linear Dichroism Spectra. *Chem. Phys.* **2010**, *373*, 110−114.
(21) Chukhutsina, V. U.; Büchel, C.; van Amerongen, H. Variations in the First Steps of Photosynthesis for the Diatom Cyclotella Meneghiniana Grown under Different Light Conditions. *Biochim. Biophys. Acta, Bioenerg.* **2013**, *1827*, 10−18.
(22) Fujita, Y.; Ohki, K. On the 710 nm Fluorescence Emitted by the Diatom *Phaeodactylum Tricornutum* at Room Temperature. *Plant Cell Physiol.* **2004**, *45*, 392−397.
(23) Kiefer, D. A. Chlorophyll a Fluorescence in Marine Centric Diatoms: Responses of Chloroplasts to Light and Nutrient Stress. *Marine Biology* **1973**, *23*, 39−46.
(24) Stehfest, K.; Toepel, J.; Wilhelm, C. The Application of Micro-FTIR Spectroscopy to Analyze Nutrient Stress-Related Changes in Biomass Composition of Phytoplankton Algae. *Plant Physiol. Biochem.* **2005**, *43*, 717−726.
(25) Furukawa, T.; Watanabe, M.; Shihira-Ishikawa, I. Green- and Blue-Light-Mediated Chloroplast Migration in the Centric Diatom *Pleurosira Laevis*. *Protoplasma* **1998**, *203*, 214−220.